

## SIMULATION-BASED STRATEGY TO DISTINGUISH BETWEEN EC(REVERSIBLE) AND EC(DIMERIZATION) MECHANISMS IN SQUARE-WAVE VOLTAMMETRY

Pavlinka Kokoškarova\*, Milkica Janeva\*

Faculty of Medical Sciences, Goce Delčev University, Štip, North Macedonia

pavlinka.kokoskarova@ugd.edu.mk milkica.janeva@ugd.edu.mk

Square-wave voltammetry (SWV) is a highly sensitive and widely used electrochemical technique, suitable for probing the kinetics of various electrochemical electrode processes coupled with different chemical reactions. However, its application to mechanisms involving subsequent chemical steps has been somewhat limited, particularly in scenarios such as those discussed in recent work.<sup>1</sup> Among the electrochemical mechanisms coupled with chemical reactions, the EC-type pathways (where an electron transfer step is followed by a reversible chemical transformation) remain fundamental for elucidating interfacial reaction dynamics. A significant variant of this mechanism is the EC(dimerization) model, which features a reversible bimolecular chemical step in which two oxidized species ( $2Ox \rightleftharpoons Ox-Ox$ ) undergo reversible dimerization, introducing second-order kinetics into the entire electrode reaction. Although mechanistically distinct, these two pathways produce similar voltammetric signatures, making them difficult to distinguish under certain experimental conditions. This challenge is further complicated by the fact that frequency modulation, a commonly used diagnostic tool in SWV, simultaneously influences both the electron transfer kinetics and the chemical reaction rate, thereby diminishing its discriminatory power. In this work, we examined the key voltammetric features of both mechanisms under SWV conditions and proposed theoretical strategies to differentiate them. Emphasis is placed on the use of numerical simulations as a robust and reliable approach for resolving mechanistic ambiguity.

**Keywords:** EC mechanism; bimolecular dimerization; voltammetry; kinetics of chemical reaction; effect of square-wave frequency

### ПРОТОКОЛ БАЗИРАН НА ВОЛТАМЕТРИСКИ СИМУЛАЦИИ ПОГОДЕН ЗА ДИСТИНКЦИЈА ПОМЕЃУ ЕС–РЕВЕРЗИБИЛЕН И ЕС–ДИМЕРИЗАЦИСКИ МЕХАНИЗАМ ВО УСЛОВИ НА КВАДРАТНО-БРАНОВА ВОЛТАМЕТРИЈА

Квадратнобрановата волтаметрија (SWV) претставува исклучително чувствителна и широко применувана електрохемиска техника, погодна за проучување на кинетиката на различни електрохемиски електродни процеси што се поврзани со дополнителни хемиски реакции. Сепак, нејзината примена кај електродни механизми што вклучуваат последователни хемиски чекори е значително ограничена, особено во сценарија какви што се дискутирани во некои понови теоретски студии.<sup>1</sup> Меѓу електрохемиските механизми спрегнати со хемиски реакции, механизмите од типот наречен „ЕС“ (каде што електронскиот трансфер „Е“ е поврзан со последователна реверзибилна хемиска трансформација „С“) претставуваат фундаментални механизми што се неопходни за објаснување на динамиката на разни интерфазни електрохемиски реакции. Многу важен поттип на електроден механизам што припаѓа во класата на ЕС–реакции е т.н. ЕС–димеризациски механизам. Кај ЕС–димеризацискиот механизам се случува реверзибилен бимолекуларен хемиски последователен чекор, во кој две оксидирани честички „Ох“ подлежат на реверзибилна димеризација ( $2Ox \rightleftharpoons Ox-Ox$ ), воведувајќи притоа кинетика од втор ред во целокупната електродна реакција. Иако механистички различни, овие два типа на ЕС механизмите даваат многу слични волтаметриски отпечатоци, што ги прави тешко да се разликуваат при одредени експериментални услови. Овој предизвик дополнително е усложнет од фактот што

квадратнобрановата фреквенција, параметар што често се користи како дијагностичка алатка во SWV, истовремено влијае и врз кинетиката на електронскиот трансфер и врз брзината на хемиската реакција и на тој начин се намалува нејзината функција за дистинкција на двата механизма. Во овој труд се испитувани клучните волтаметриски карактеристики на двата механизма во услови на SWV, при што се предложени теоретски стратегии за дистинкција на двата електродни механизма. Посебен акцент е ставен на употребата на нумерички симулации како робустен и ефикасен пристап кон решавање на механистичките проблеми кај овие електрохемиски механизми.

**Клучни зборови:** EC–електроден механизам; бимолекуларна димеризација; волтаметрија; кинетика на хемиски реакции; ефект на квадратнобрана фреквенција

## 1. INTRODUCTION

Electrochemical reactions coupled with follow-up chemical reactions – commonly referred to as EC mechanisms<sup>1</sup> – play an important role in understanding the redox behavior of numerous systems, particularly in biological and physiological contexts.<sup>2</sup>

In living organisms, many redox-active biomolecules (redox proteins, redox enzymes, neurotransmitters, quinones, vitamins, and various metabolite products) undergo electron transfer steps that are coupled with reversible chemical reactions, most commonly involving protonation-deprotonation equilibria.<sup>3,4</sup>

These reactions modulate not only the thermodynamics and kinetics of the associated redox processes but also their biological functions and signaling capabilities. For example, the redox activity of quinones, catecholamines, flavins, and proteins containing amino acid residues like tyrosine or cysteine is often regulated by proton-coupled electron transfer, serving as archetypal examples of EC mechanisms in biological redox chemistry.<sup>2-6</sup>

The coupling of electron transfer with protonation or other reversible chemical steps shapes the electrochemical signatures of these molecules and governs their behavior under physiological conditions.

Beyond EC pathways coupled with protonation equilibria, a distinct class of EC mechanisms emerges when reactive intermediates – such as radicals – are generated through an electron exchange step. These radical species often exhibit high reactivity and commonly undergo bimolecular dimerization, leading to the formation of stable or metastable dimers.

This class of mechanisms, known as EC(dimerization) systems, is particularly relevant in organic and bioinorganic redox chemistry, where radical–radical interactions are widespread.<sup>7,8</sup> Examples include phenoxyl radicals derived from

tyrosine, semiquinone species, and radical forms of certain neurotransmitters and antioxidants.<sup>8,9</sup>

Although these reactions may resemble, under voltammetric conditions, the more familiar EC mechanisms involving unimolecular chemical steps, they differ fundamentally in their kinetic order. While a simple EC mechanism typically involves a first-order chemical transformation, EC(dimerization) mechanisms follow second-order kinetics due to the bimolecular nature of the dimerization step.

This distinction results in notable differences in their voltammetric profiles, particularly when EC mechanisms are investigated using dynamic electrochemical techniques. Over the past several decades, significant theoretical advances have been made in the interpretation and modeling of various EC mechanisms<sup>1,2,6,10-14</sup> using different voltammetric techniques. Pioneering work by Nicholson and Shain<sup>11</sup> in the 1960s laid the groundwork for understanding electrochemical–chemical sequences in cyclic voltammetry. Subsequent developments by Compton,<sup>6,12,13</sup> Lovric,<sup>14</sup> Molina,<sup>15</sup> and others<sup>1,16,17</sup> expanded this framework to pulse voltammetric techniques, incorporating reversible and irreversible chemical steps.

In the context of square-wave voltammetry (SWV), which is one of the most advanced pulse techniques available, many researchers have developed detailed mathematical models and simulation protocols for complex EC-type systems.<sup>12-18</sup> These works have revealed that although EC(reversible) and EC(reversible dimerization) mechanisms share some general features – such as peak current dependencies and potential shifts as a function of chemical kinetic parameters – their detailed behaviors differ due to their different kinetic orders, especially in terms of current profiles and peak potential evolution.

In this context, distinguishing between these two types of EC mechanisms under square-wave voltammetric conditions is critically important. Accurate mechanistic assignment has profound

implications for interpreting redox processes in organic synthesis, studying catalytic reactions, and analyzing various biological systems. Moreover, understanding whether a defined electrochemical system proceeds via a simple reversible chemical step or through a dimerization pathway directly impacts the estimation of kinetic and thermodynamic parameters, such as rate constants and equilibrium constants.

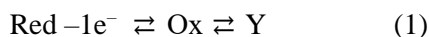
Given the complex interplay between frequency, electron transfer kinetics, and chemical rate parameters in SWV,<sup>1,17</sup> traditional approaches to mechanistic discrimination often fall short. Thus, there is a pressing need for new theoretical and experimental protocols capable of unambiguously distinguishing EC(reversible) mechanisms<sup>14,17</sup> from EC(reversible dimerization)<sup>18</sup> pathways under the specific dynamic perturbations introduced by square-wave voltammetry.

To address this need, we present a series of theoretical results that aim to resolve this problem.

## 2. THEORETICAL MODELS

Two well-established theoretical models derived from the EC mechanistic scheme were investigated under the conditions of square-wave voltammetry.

The first model is represented by the reaction scheme (1):



and is denoted as the EC(reversible) mechanism, where the follow-up step is assumed to be a first-order reversible chemical reaction.

The second model is represented by the reaction scheme (2):



and is referred to as the EC(reversible dimerization) mechanism (or simply, ECdimerization), involving a bimolecular chemical step between two oxidized species. "Red" and "Ox" stay for the reduced and oxidized forms of the electrochemically active species involved in the electrochemical transformation, respectively. The voltammetric responses of both mechanisms are analyzed under the conditions of a semi-infinite planar diffusion model at a stationary electrode, using the Butler-Volmer kinetic formalism.

The voltammetric features of both mechanisms are primarily governed by three key dimensionless parameters. The first is the dimensionless rate parameter of electron transfer,  $K$ , defined as  $K$

$= k_s^\ominus (Df)^{-0.5}$ . The dimensionless parameter  $K$  couples the heterogeneous electron transfer rate constant  $k_s^\ominus$  with the rate of diffusion (expressed via the diffusion coefficient  $D$ ) and the square-wave frequency  $f$ . This definition provides insight into the interplay between electron transfer kinetics and mass transport relative to the time scale of current measurement in SWV.

The second dimensionless parameter in both models is the equilibrium constant of the chemical step,  $K_{\text{eq}}$ , while the third is the dimensionless chemical rate parameter,  $K_{\text{chem}}$ , which captures the kinetic activity of the coupled homogeneous chemical step relative to the timescale of the square-wave perturbation.

The definitions of  $K_{\text{eq}}$  and  $K_{\text{chem}}$  for the EC mechanism involving a first-order chemical reaction are identical to those reported in references,<sup>14,17,19</sup> while the corresponding parameters for the EC mechanism incorporating a reversible dimerization step are defined as described in reference.<sup>18</sup>

Together with temperature ( $T$ ), square-wave potential signal parameters (potential step  $dE$ , amplitude  $E_{\text{sw}}$ , and frequency  $f$ ), and the electron transfer coefficient  $\alpha$ , these three dimensionless parameters define the key features of the simulated voltammetric profiles.

The theoretical basis for the EC(reversible) mechanism under SWV conditions is detailed in references,<sup>14,17,19</sup> while the EC(reversible dimerization) model is developed and elaborated in reference.<sup>18</sup>

## 3. RESULTS AND DISCUSSION

### 3.1. Effect of the dimensionless chemical parameter ( $K_{\text{chem}}$ ) on the features of the square-wave voltammetric profiles of EC(reversible) and EC(dimerization) mechanisms

In the context of gaining insight into the crucial differences between both mechanisms, it was appropriate to start with a comparison of the square-wave voltammetric profiles of the EC(reversible) mechanism and the EC(reversible dimerization) mechanism, calculated as a function of the dimensionless chemical parameter  $K_{\text{chem}}$ .

The simulation profiles displayed in Figure 1 represent a series of square-wave voltammograms (forward and backward current components) calculated for an EC(reversible) electrode mechanism under the conditions of fast electron transfer kinetics and a large equilibrium constant ( $K_{\text{eq}}$ ) for the follow-up chemical reaction.

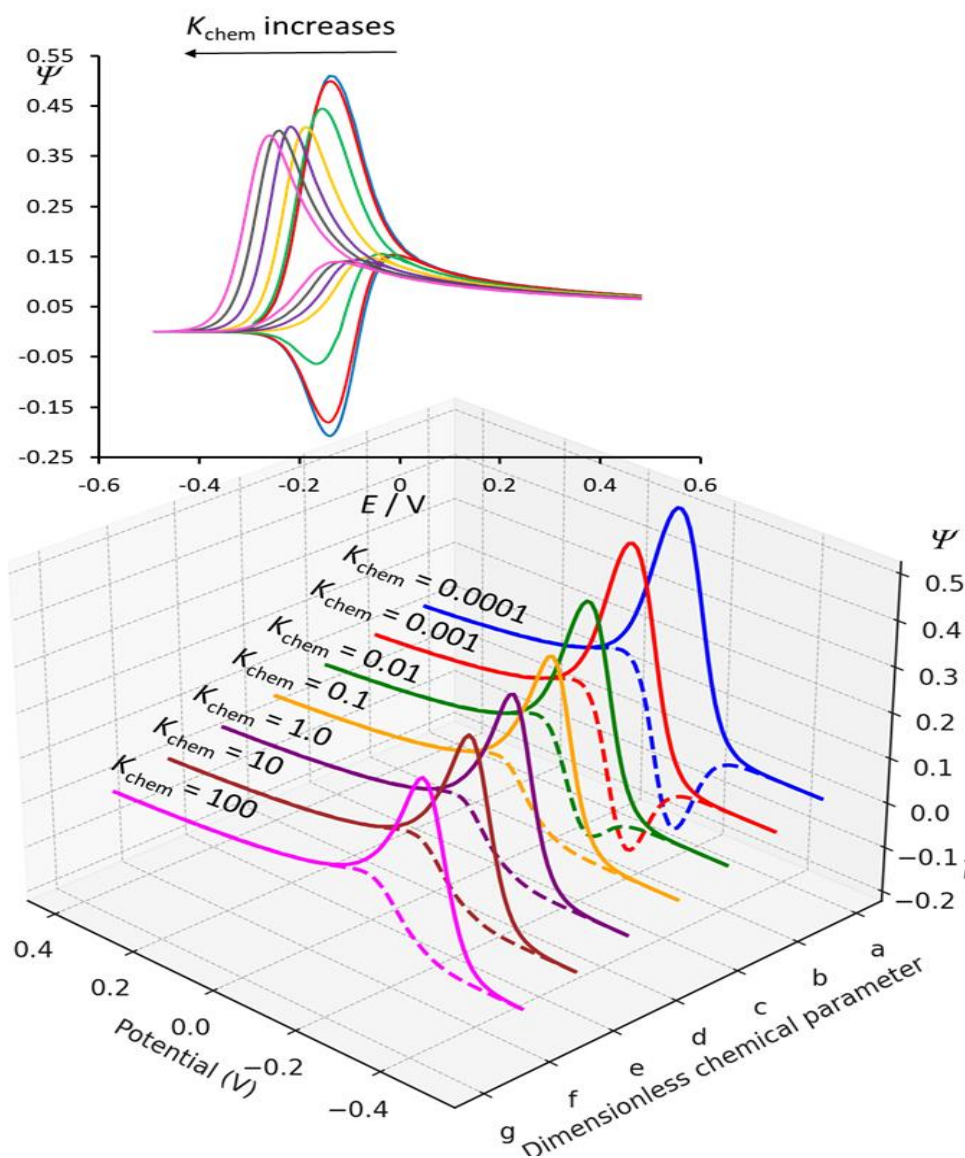


**Fig. 1.** Forward and backward current components of SWV responses for an EC (reversible) mechanism were simulated as a function of the dimensionless chemical rate parameter  $K_{\text{chem}}$ . The simulations were conducted under the following conditions: dimensionless electron transfer kinetic parameter  $K = 31$ , electron transfer coefficient  $\alpha = 0.5$ , temperature  $T = 298$  K, square-wave amplitude  $E_{\text{sw}} = 50$  mV, and potential step  $dE = 10$  mV. The equilibrium constant of the subsequent chemical reaction was fixed at  $K_{\text{eq}} = 100$ .  $K_{\text{chem}}$  values used in the simulations are indicated in the 3D voltammogram plot. The 2D voltammograms presented in the upper panel correspond exactly to the profiles depicted in the 3D graph. Starting potential was set to  $-0.5$  V.

This set of simulations was performed with a fixed dimensionless rate parameter of electron transfer  $K = 31$ , for  $\alpha = 0.5$ , and an equilibrium constant  $K_{\text{eq}} = 100$ , while systematically varying the dimensionless chemical parameter  $K_{\text{chem}}$  from 0.0001 up to 100.

As previously mentioned, the dimensionless chemical parameter  $K_{\text{chem}}$  unified the rate of follow-up chemical reaction with the time resolution (i.e., the square-wave frequency) of the applied square-wave pulses. As illustrated by the simulated voltammograms shown in Figure 1, a progressive increase in the magnitude of  $K_{\text{chem}}$  resulted in a

notable shift of the entire voltammogram signal toward more negative potentials. This phenomenon was observed in both the forward and backward current components, and it became increasingly pronounced as the chemical reaction accelerated.

From a mechanistic point of view, this behavior was attributed to the dynamic depletion of the electrochemically generated intermediate species (Ox) by the fast and reversible chemical reaction that followed the electron-transfer step. As the chemical step became more kinetically dominant in the entire mechanism (1), Ox was removed more rapidly from the interfacial region, thus disrupting

the local equilibrium at the electrode/electrolyte interface. This depletion of Ox drove the oxidation process (electrode transformation of Red to Ox) more efficiently, while requiring a lower applied potential to sustain the same current response.

In addition to this shift in peak potential, significant changes were observed in the reverse (reduction) current component of the square-wave voltammograms. For small values of  $K_{\text{chem}}$ , the backward peak was distinct and symmetric to the forward one, reflecting the availability of Ox for reduction during the reverse pulse. However, as the chemical reaction became faster, the backward peak progressively diminished and was eventually suppressed. This suppression occurred because the Ox species was rapidly converted into the chemically stable product Y during the forward pulse. As a result, there was insufficient Ox remaining to be reduced, and the backward current became negligible.

From both a kinetic and thermodynamic perspective, the scenario depicted in the voltammograms of Figure 1 illustrated the strong coupling between the electron-transfer event and the follow-up chemical transformation. The high equilibrium constant ensured that the chemical conversion of Ox to Y was thermodynamically favored, while increasing  $K_{\text{chem}}$  ensured that the follow-up chemical transformation occurred rapidly on the voltammetric timescale.

Together, these conditions led to a pronounced distortion in the voltammetric response, characterized by negative peak potential shifts in the entire voltammetric profile and substantial attenuation of the backward signal. These features were commonly used as voltammetric diagnostics for EC-type mechanisms where the intermediate was actively consumed by a reversible chemical transformation.<sup>1,11,14,17,19</sup>

Shown in Figure 2 is a series of working curves illustrating the dependencies of the net peak potentials ( $E_{\text{net,p}}$ ) of square-wave voltammograms for an EC(reversible) electrode mechanism, plotted as a function of  $\log(K_{\text{chem}})$ . The curves were evaluated at several magnitudes of the equilibrium constant  $K_{\text{eq}}$ , and were displayed within the plot. In all cases, the working curves exhibited typical sigmoidal features, which have been widely recognized in theoretical analyses of kinetically coupled electrochemical reactions.<sup>1,14,17,19</sup>

For every value of  $K_{\text{eq}}$ , the progression of the peak potential values with respect to  $\log(K_{\text{chem}})$  followed a trend with three features: a) plateau at low chemical reactivity; b) a linear region at intermediate  $K_{\text{chem}}$ ; and c) a second plateau at high chemical rates. The most prominent feature in all of the curves lay in the linear mid-region, which marked the kinetic regime where the chemical step increasingly influenced the electrochemical response.

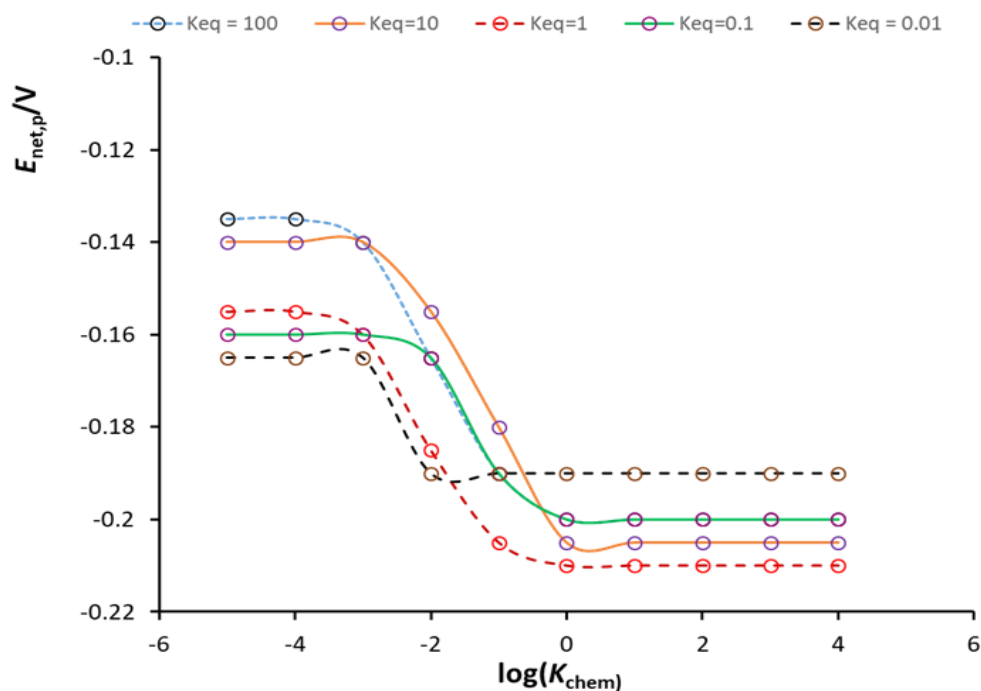


**Fig. 2.** Dependence of the peak potentials of net square-wave voltammograms ( $E_{\text{net,p}}$ ) of an EC(reversible) mechanism as a function of  $\log(K_{\text{chem}})$ . Working curves are constructed at several values of equilibrium constant of follow up chemical reaction ( $K_{\text{eq}}$ ), whose values are given in the graph. Other simulation conditions were same as those in Figure 1.

As shown in Figure 2, the extent and slope of these linear segments were critically dependent on the magnitude of  $K_{\text{eq}}$ . For larger values (e.g.,  $K_{\text{eq}} \geq 10$ ), the sigmoidal curve was more extended, and the linear kinetic region spanned over a broader range of  $K_{\text{chem}}$ . This result indicated that for highly favorable chemical equilibria, the EC mechanism remained sensitive to kinetic modulations over a wider domain of chemical reaction rates. In contrast, as the magnitude of  $K_{\text{eq}}$  decreased (e.g.,  $K_{\text{eq}} \leq 0.5$ ), the sigmoidal curves became compressed, and the linear region narrowed, which indicated that the influence of the chemical reaction rate on the peak potential was confined to a smaller kinetic window.

A particularly important theoretical insight was the slope of the linear portion of these sigmoidal plots, which remained consistently around  $-30$  mV per decade increase in  $K_{\text{chem}}$ , regardless of the magnitude of  $K_{\text{eq}}$ . This characteristic slope had been previously discussed and validated in the works of Lovric<sup>14,17</sup> and Osteryoung,<sup>19</sup> who identified it as one of the hallmarks of the EC(reversible) mechanism under square-wave voltammetric conditions. The  $-30$  mV/ $\log(K_{\text{chem}})$  behavior reflected the fact that the chemical step, although reversible, modified the electrochemical potential distribution at the electrode interface in an almost Nernstian (thermodynamically reversible) manner when the system was under kinetic control of chemical reaction.

Similar voltammetric patterns (from a qualitative perspective) were obtained for the EC(dimerization) mechanism, as presented in Figure 1. Additionally, Figure 3 showcased a series of square-wave voltammograms calculated for an EC(reversible dimerization) electrode mechanism under conditions of fast electron transfer (with dimensionless parameter  $K = 31$ ) and a large equilibrium constant for the follow-up chemical step ( $K_{\text{eq}} = 100$ ).

These simulations were conducted under identical conditions to the EC(reversible) case, with the chemical rate parameter  $K_{\text{chem}}$  again varied over a wide range (from 0.0001 for the blue curve to 100 for the magenta curve). This configuration permitted a direct comparative analysis between the voltammetric behavior of the EC(reversible dimerization) mechanism and the simpler EC(reversible) mechanism involving a first-order chemical reaction.

A key observation from the voltammetric profiles displayed in Figure 3 was the stronger and more pronounced shift of the voltammetric profiles toward more negative potentials as the magnitude of  $K_{\text{chem}}$  increased. This effect was significantly more intense than what was observed in the EC(reversible) mechanism. The more pronounced negative shift of the net peak potential of SW voltammograms displayed in Figure 3 reflected a much easier oxidation process under these conditions, which was a consequence of the second-order nature of the follow-up chemical reaction.

In the electrode mechanism involving a chemical dimerization scenario, two molecules of the electrochemically generated Ox species were consumed simultaneously in the chemically reversible formation of a dimeric product. This consumption resulted in a quadratic depletion of the Ox species with respect to its concentration, thus making the system kinetically "more aggressive" in removing Ox from the interfacial zone, even at relatively modest values of  $K_{\text{chem}}$ .

From a kinetic perspective, the faster consumption of Ox via dimerization rapidly shifted the dynamic equilibrium of the electron transfer step ( $\text{Red} - 1e^- \rightleftharpoons \text{Ox}$  sequence) in the direction of an easier oxidation. This effect drove the electrode reaction forward more effectively and caused the system to reach its oxidative state at lower applied potentials. The more intensive the rate of the dimerization reaction was (i.e., the higher the magnitude of  $K_{\text{chem}}$ ), the stronger this potential shift became.

Additionally, the backward (reduction) components of the voltammograms were dramatically affected by this second-order chemical step. As the magnitude of  $K_{\text{chem}}$  increased, the Ox species was consumed more rapidly than at the "simple" EC(reversible) mechanism, so only minute amounts of Ox remained available for reduction during the current-measuring time of the reverse pulse. This Ox depletion resulted in an almost complete disappearance of the backward peak current, even at much lower magnitudes of  $K_{\text{chem}}$  (evident in the orange- to magenta-colored curves in Fig. 3). The voltammograms became increasingly asymmetric, even at moderate magnitudes of  $K_{\text{chem}}$ , highlighting the decoupling of the redox couple under strong kinetic constraints.

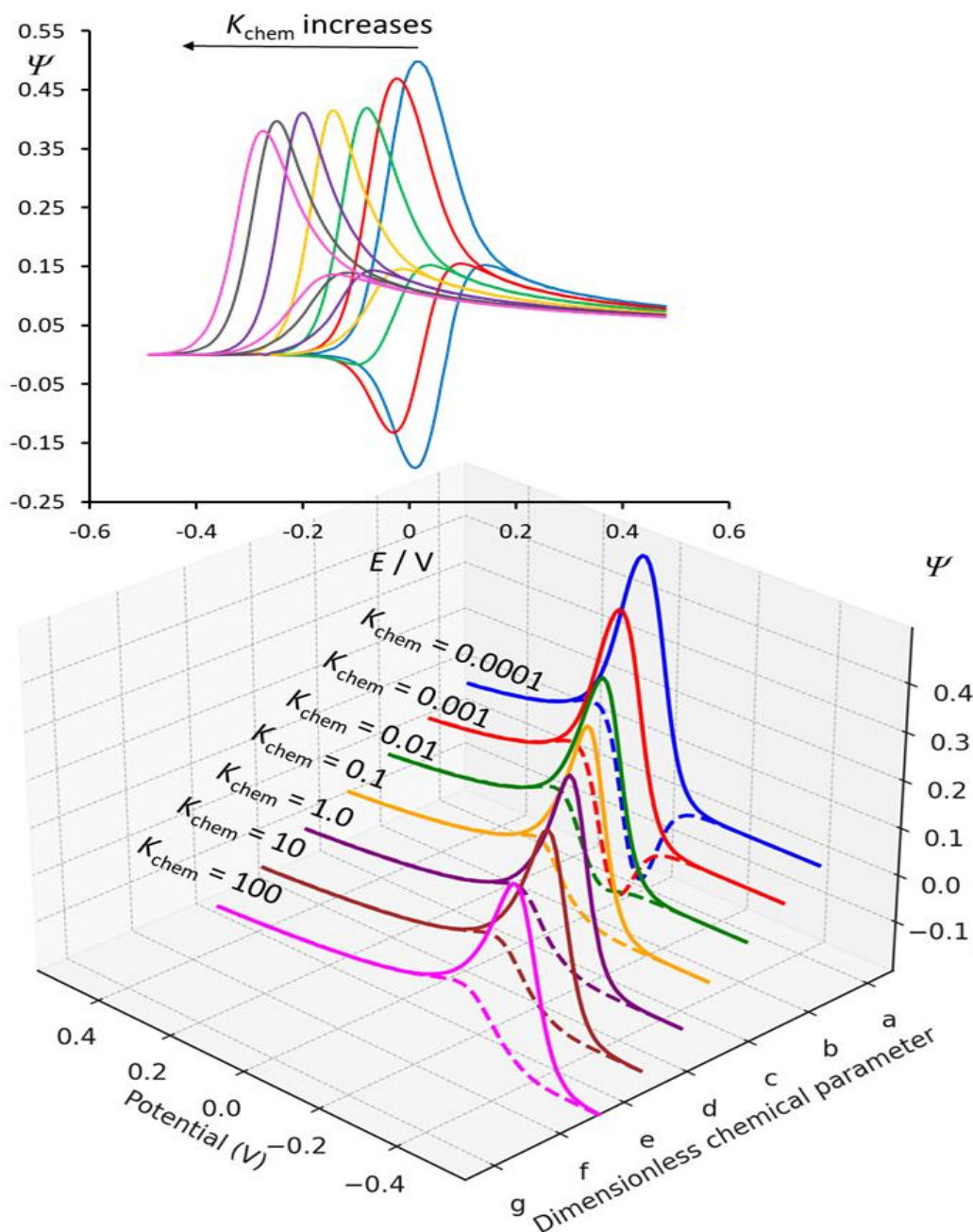


**Figure 3.** Forward and backward current components of square-wave voltammetric profiles for an EC(dimerization) mechanism simulated as a function of the dimensionless chemical rate parameter  $K_{\text{chem}}$ . The 2D voltammograms presented in the upper panel correspond to the profiles depicted in the 3D graph. All other simulation parameters were identical as those reported in Figure 1.

Figure 4 showcased a series of working curves representing the dependence of the net peak potentials of square-wave voltammograms simulated for an EC(dimerization) mechanism plotted against the logarithm of the chemical rate parameter  $\log(K_{\text{chem}})$ . The working curves were evaluated for various values of the chemical equilibrium constant  $K_{\text{eq}}$ .

As in the previous case (see Fig. 2), the working curves exhibited distinct sigmoidal shapes, char-

acteristic of systems where a chemically coupled step progressively influenced the electrochemical behavior as its rate increased. These profiles, however, displayed specific features that distinguished them markedly from the simpler EC(reversible) mechanism. A notable difference was observed in the significantly broader linear kinetic regions within the sigmoidal curves of the dimerization mechanism.

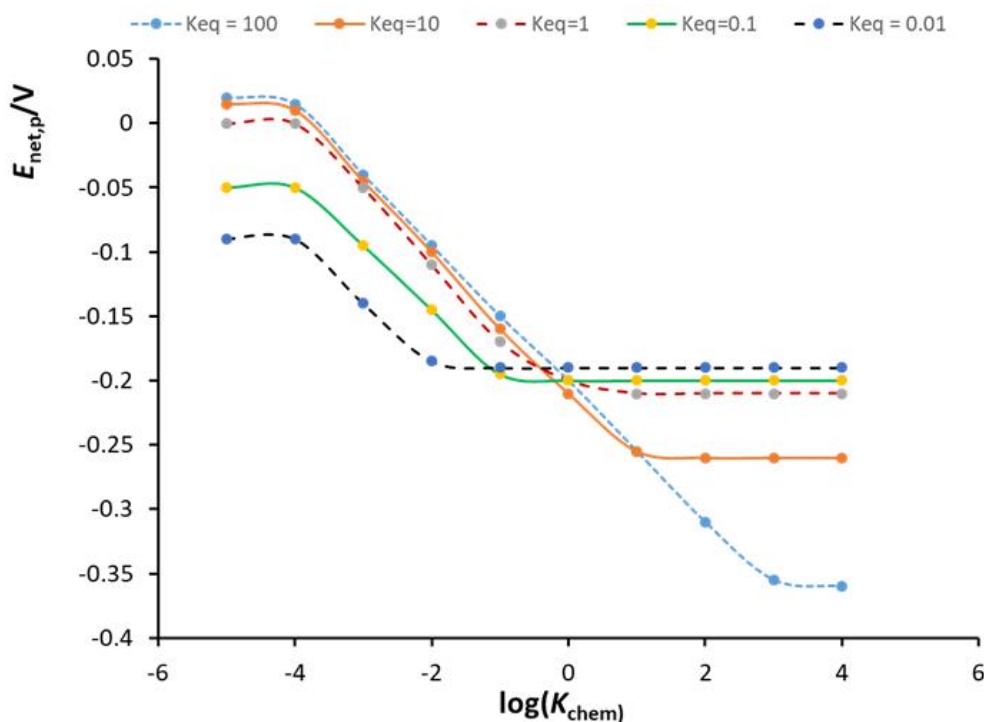


**Fig. 4.** Dependence of the peak potentials of net square-wave voltammograms ( $E_{\text{net,p}}$ ) of an EC(dimerization) mechanism as a function of  $\log(K_{\text{chem}})$ . Working curves are constructed at several values of equilibrium constant of follow up chemical reaction, whose values are given in the graph. Other simulation conditions were same as those in Figure 1.

As  $K_{\text{chem}}$  increased, each curve entered a domain in which the peak potential shifted nearly linearly with the logarithm of the chemical parameter. These linear ranges spanned a much wider domain compared to the EC(reversible) case (see the curves in Fig. 4 and compare with the corresponding profiles in Fig. 2), indicating that the voltammetric response remained sensitive to changes in chemical kinetics over a broader range of time scales. This behavior arose from the second-order nature of the follow-up dimerization reaction, in which the electrochemically generated species Ox participated in a bimolecular transformation ( $2\text{Ox} \rightleftharpoons \text{Ox-Ox}$ ). As such, the rate of Ox depletion depended quadratically on its concentration, which led to more efficient consumption of Ox, and thus a more pronounced shift in the electrode potential.

Another important observation was the dependency of the linear region's extent on the value of  $K_{\text{eq}}$ . As  $K_{\text{eq}}$  increased, the linear segment became more extended, covering several orders of magnitude of  $K_{\text{chem}}$ . This extension reflected the thermodynamic driving force of the chemical step: a larger equilibrium constant promoted more complete conversion of Ox into Y, thereby amplifying the impact of chemical kinetics on the voltammetric signal. Conversely, for smaller  $K_{\text{eq}}$  values, the

chemical step was less thermodynamically favored, and the influence of  $K_{\text{chem}}$  was confined to a narrower range.

It is important to note that the slope of the linear segments in all these sigmoidal dependencies presented in Figure 4 was approximately  $-60$  mV per decade increase in the magnitude of  $K_{\text{chem}}$ .<sup>20</sup> This slope was roughly double that of the slope observed for the EC(reversible) mechanism, where the shift was typically around  $-30$  mV/decade (see Fig. 2).<sup>19</sup>

The steeper slope in the dimerization case directly resulted from the second-order chemical kinetics, where two Ox species were consumed per chemical event. This quadratic dependency enhanced the effect of increasing  $K_{\text{chem}}$  on the system's electrochemical behavior, and thus doubled the rate at which the peak potential shifted with respect to changes in the chemical rate.

### 3.2. Role of SW frequency modulation in both mechanisms

Although both EC(reversible) and EC(reversible dimerization) mechanisms considered in this work may have appeared similar in their overall structure, some important differences in their voltammetric behavior emerged under SWV conditions, which were critical for accurate mechanistic interpretation.

The chemical reactions involved in the considered mechanisms were of different order with respect to the concentration of the electrochemically generated species "Ox". However, since the concentration "Ox" was not controllable during the electrochemical experiment (i.e., "Ox" was generated *in situ*), the concentration of "Ox" could not be considered a relevant variable in assessing the effect of the dimensionless chemical rate parameter by either mechanism.

Therefore, a challenging situation arose in developing a relevant diagnostic protocol capable of distinguishing these two mechanisms, particularly because the other controllable parameter – the SW frequency – simultaneously affected the kinetics of all steps involved in both electrode mechanisms.

One of the most distinguishing features of the EC(dimerization) mechanism in SWV was the rapid suppression of the backward current peak. As chemical dimerization was a second-order reaction, the oxidized species (Ox) was consumed via dimer formation, especially at higher concentrations of Ox generated during the forward SW pulse. This additional consumption resulted in a more pronounced suppression of the backward peak compared to the EC(reversible) mechanism, where the unimolecular transformation ( $\text{Ox} \rightleftharpoons \text{Y}$ ) occurred.

Therefore, the steeper decline of backward peak currents was one of the notable hallmarks of the dimerization route. However, this criterion could not be regarded as reliable, as differing rate constants of the chemical reactions in both mechanisms could lead to misinterpretation when attempting to distinguish the EC(dimerization) mechanism from the simple EC(reversible) mechanism.

A more important distinguishing feature, as demonstrated in Figures 2 and 4, was the dependence of the peak potentials of voltammetric profiles on the rate of the chemical reaction in both mechanisms. In EC(reversible), the net peak potential shifted approximately by  $-30$  mV per decade change in the logarithm of the dimensionless chemical rate parameter, while in EC(reversible dimerization), this shift was steeper, approaching  $-60$  mV per decade increase in  $K_{\text{chem}}$ . Moreover, the length of the kinetic region – the range of chemical rate constants over which the voltammetric response transitioned from reversible to quasi-reversible or irreversible behavior – was significantly broader in EC(dimerization).

Despite the appeal of frequency modulation as an important diagnostic tool in SWV,<sup>1,17</sup> its role in mechanistic distinction between EC(reversible) and EC(dimerization) mechanisms was rather limited. This limitation occurred because the frequen-

cy appeared in the definition of both the dimensionless chemical parameter ( $K_{\text{chem}}$ ) and the dimensionless parameter related to the rate of electron transfer step ( $K$ ). Specifically, the chemical parameter was inversely proportional to the SW frequency (e.g.,  $K_{\text{chem}} = \varepsilon/f$ ), while the electron transfer rate parameter was defined by  $K = k_s^\circ/(Df)^{0.5}$ . As a result, changing the frequency altered both the rate of chemical transformation and the dynamics of electron transfer (see Fig. 5)<sup>17</sup> in a coupled and inseparable manner.<sup>1,17</sup>

This dual dependence created a confounding effect since any observed shift in peak potential or change in peak current with frequency could no longer be attributed solely to the kinetics of the chemical reaction. Consequently, frequency lost its diagnostic specificity and could not be used to distinguish between EC(reversible) and EC(dimerization) mechanisms in a conclusive manner. Furthermore, the simultaneous alteration of both chemical and electron transfer kinetics obscured the true mechanistic behavior, especially in intermediate kinetic regimes of the curves presented in Figures 2 and 4.

It is worth mentioning that decreasing the SW frequency induced an increase in the apparent reversibility of voltammetric profiles when studying the effect of  $K$ . At the same time, however, the decrease in SW frequency led to an increase in the dimensionless chemical parameter, which resulted in greater irreversibility of voltammetric profiles. These two effects were opposite and could lead to misinterpretations of the obtained voltammetric results.

Nevertheless, under certain conditions, frequency modulation still offered limited utility in distinguishing between these two mechanisms. Notably, since the frequency dependence of  $K_{\text{chem}}$  was  $f^{-1}$ , while that of  $K$  was  $f^{-0.5}$ , variations in frequency had a more pronounced effect on the rate of the chemical step than on the electron transfer process. Therefore, if the electron transfer was sufficiently fast, quantified by  $\log(K) > 1$ ,<sup>17</sup> corresponding to a regime of rapid interfacial electron exchange, then frequency modulation in the range of approximately 0.1 Hz to 200 Hz could selectively influence the chemical kinetics. In such cases, one could observe a characteristic shift in peak potential of either  $-30$  mV or  $-60$  mV per decade modulation in frequency magnitude, corresponding to a first-order or second-order chemical step (dimerization), respectively. This observation could serve as a diagnostic criterion to distinguish between EC(reversible) and EC(reversible dimerization) mechanisms.

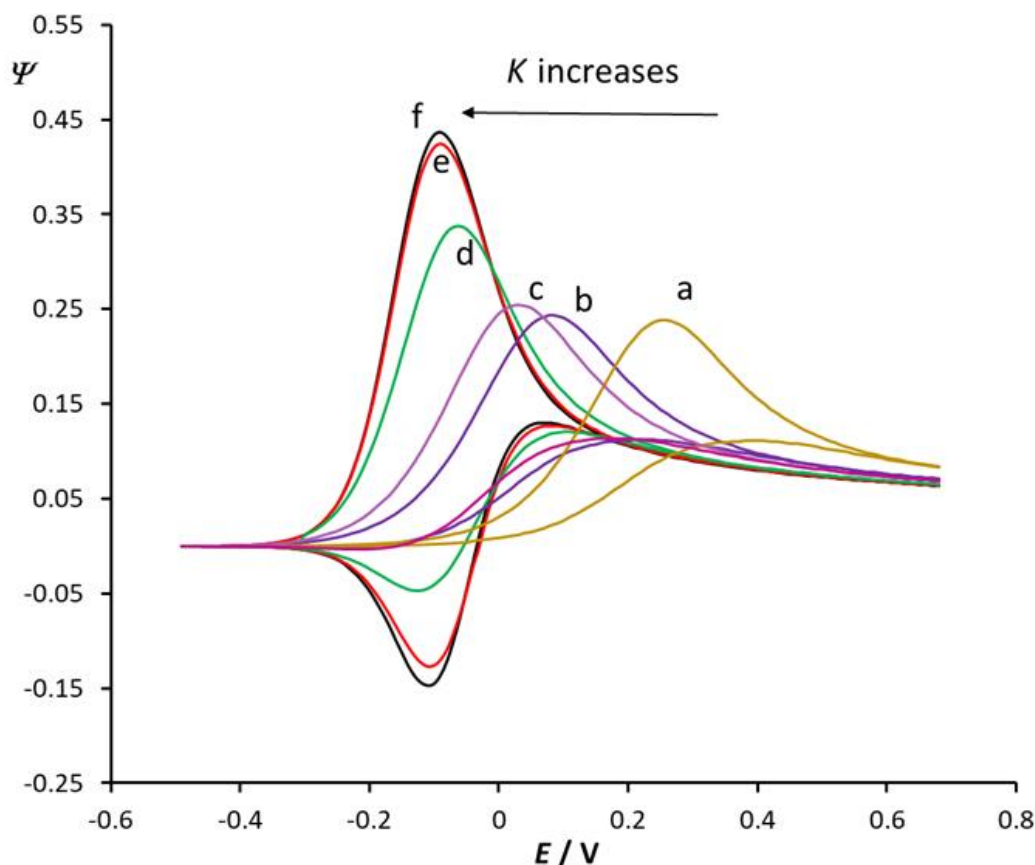


**Figure 5.** Forward and backward square wave voltammetric profiles of a simple Red  $- 1e^- \rightleftharpoons$  Ox diffusional mechanism simulated as a function of dimensionless kinetic parameter of electrode reaction  $K$ . Values of  $K$  were set to 0.005 (a), 0.05 (b), 0.09 (c), 0.5 (d), 2.25 (e) and 22.5 (f). Other simulation parameters were identical as those reported in Figure 1.

However, to implement such an approach, it was essential to first determine the standard heterogeneous electron transfer rate constant  $k_s^\ominus$ , which could be estimated using established experimental protocols.<sup>21</sup>

Once the value of  $k_s^\ominus$  was known and fell in range above  $1 \text{ cm s}^{-1}$ , and if the values of the diffusion coefficient and the electron transfer coefficient  $\alpha$  were also available (or determined),<sup>17</sup> one could proceed to a fitting procedure between experimental and theoretical SW voltammograms. Theoretical frameworks for EC(reversible) and EC(reversible dimerization) mechanisms were available in the works of Garay and Lovric<sup>14</sup> and Lovric, Jadresko, and Komorsky-Lovric,<sup>18</sup> respectively. Additionally, a voltammetric profile fitting process enabled quantitative extraction of the kinetic and thermodynamic parameters related to the follow-up chemical reaction, as well as the kinetics of the electron transfer step.

When the fitting procedure between theoretical and experimental voltammetric patterns was applied, it was advisable to fit the normalized forward and backward current components of both

voltammetric responses. Such a fitting procedure was always useful, as it avoided certain artifacts (e.g., parasitic currents) that commonly appeared in experimental voltammograms.

It is also worth mentioning that alongside variation of SW frequency, we attempted to explore the square-wave amplitude as a tool to distinguish between both mechanisms. Although changing the square-wave amplitude might have enabled potential distinction between the two mechanisms, our analyses revealed that the amplitude of SW pulses had shown an almost identical effect in both mechanisms.

#### 4. CONCLUSION

While square-wave voltammetry offered a powerful window into the kinetics of various electrochemical systems, the ability to discriminate between EC(reversible) and EC(dimerization) mechanisms required careful consideration of the interdependent variables involved.

The conventional approach of frequency modulation in SWV was often insufficient and

even somewhat misleading, due to its simultaneous influence on both chemical and electron transfer rates. It should be emphasized, however, that a frequency-based diagnostic approach was valid under conditions where the electron transfer occurred very rapidly.

In kinetic regimes dominated by the electron transfer step – specifically when electron transfer fell in the quasi-reversible region – frequency affected both the electrode transfer and the chemical reaction rates in an inseparable manner. Conversely, in cases of very slow electron transfer, the rate of the chemical reaction had a negligible effect on the voltammetric profile, as extensively discussed in the initial work by Osteryoung.<sup>19</sup> As a result, mechanistic resolution under such conditions became unreliable when relying solely on frequency analysis.

An alternative method for distinguishing the two mechanisms considered in this work was recognized in reference,<sup>18</sup> where the authors examined the dependence peak potential on the bulk concentration of the initial electroactive species present in the electrochemical cell. However, the model-based simulation approach reported in this study proved to be most reliable – not only for differentiating between these two similar mechanisms but also for accessing all parameters relevant to each.

The procedure for simulations of an EC(reversible) mechanism in SWV was provided in reference,<sup>17</sup> while the protocol for simulating EC(reversible dimerization) in SWV was outlined in reference.<sup>18</sup>

Both theoretical model protocols for EC(reversible) and EC(dimerization) mechanisms in MATHCAD format – ready for simulations – are available upon request from the authors, and they are also available at the Repository of our university.

By following strategies developed in this work and by utilizing the simulation protocols for EC(reversible)<sup>17</sup> and EC(dimerization)<sup>18</sup> mechanisms, one could even develop an analytical protocol capable of uncovering the true nature of coupled electrochemical systems under various dynamic SWV conditions.<sup>22,23</sup>

## REFERENCES

- (1) Gulaboski, R.; Mirceski, V.; Lovric, M., Critical aspects in exploring time analysis for the voltammetric estimation of kinetic parameters of surface electrode mechanisms coupled with chemical reactions, *Maced. J. Chem. Chem. Eng.* **2021**, *40*, 1–10. DOI: 10.20450/mjce.2021.2270
- (2) Saveant, J. M.; Costent, C., *Elements of Molecular and Biomolecular Electrochemistry: An Electrochemical Approach to Electron-Transfer Chemistry*, 2<sup>nd</sup> ed. John Wiley & Sons, **2006**.
- (3) Kokoskarova, P.; Ruskovska, T.; Brycht, M.; Skrzypek, S.; Mirceski, V., Label-free voltammetric screening of human blood serum, *Maced. J. Chem. Chem. Eng.* **2024**, *43*, 49–59. DOI: 10.20450/mjce.2024.2859
- (4) Lewenstam, A.; Gorton, L.; Wieckowski, A., *Electrochemical Processes in Biological Systems*. The Wiley Series on Electrocatalysis and Electrochemistry, Wiley, **2015**.
- (5) Asche, C., Antitumour quinones. *Mini Rev. Med. Chem.* **2005**, *5*, 449–467. DOI: 10.2174/1389557053765556
- (6) Compton, R. G.; Banks, C. E., *Understanding Voltammetry*, 2<sup>nd</sup> ed. Imperial College Press, London, **2011**.
- (7) Commoner, B.; Townsend, J.; Pake G. E., Free radicals in biological materials, *Nature*, **1954**, *174*, 689–691. <https://doi.org/10.1038/174689a0>
- (8) Halliwell, B.; Gutteridge J. M. C., *Free Radicals in Biology and Medicine*. 2nd ed. Oxford, Clarendon Press, **1989**.
- (9) Nordberg, J.; Arner E. J., Reactive oxygen species, anti-oxidants, and the mammalian thioredoxin system, *Free Radical Biol. Med.* **2001**, *31*, 1287–312. DOI: 10.1016/s0891-5849(01)
- (10) Eswari, A.; Rajendran, L., Mathematical modeling of cyclic voltammetry for EC reaction, *Russ. J. Electrochem.* **2011**, *47*, 181–190. <https://doi.org/10.1134/S1023193511020078>
- (11) Nicholson, R. S.; Shain, I., Theory of stationary electrode polarography. Single scan and cyclic methods applied to reversible, irreversible, and kinetic systems, *Anal. Chem.* **1964**, *36*, 706–723. <https://doi.org/10.1021/ac60210a007>
- (12) Brokes, B. A.; Compton, R. G., Simulation of square-wave voltammetry: Quasi-reversible electrode processes, *J. Phys. Chem. B* **1999**, *103*, 9020–9028. <https://doi.org/10.1021/jp991508v>
- (13) Miles, A. B. Compton, R. G., Simulation of square-wave voltammetry: EC and ECE electrode processes. *J. Phys. Chem. B* **2000**, *104*, 5331–5342. <https://doi.org/10.1021/jp0006882>
- (14) Garay, F.; Lovric, M., Square-wave voltammetry of quasi-reversible electrode processes with coupled homogeneous chemical reactions, *J. Electroanal. Chem.* **2002**, *518*, 91–102. [https://doi.org/10.1016/S0022-0728\(01\)00695-7](https://doi.org/10.1016/S0022-0728(01)00695-7)
- (15) Molina, A.; Lopez-Tenes, M.; Laborda, E., Unified theoretical treatment of the Eirrev, CE, EC and CEC mechanisms under voltammetric conditions, *Electrochem. Commun.* **2018**, *92*, 48–55. <https://doi.org/10.1016/j.elecom.2018.03.011>
- (16) Bard, A. J.; Faulkner, R. A., *Electrochemical Methods: Fundamentals and Applications*, 2nd ed. Wiley, New York, **2011**.
- (17) Mirčeski, V.; Komorsky-Lovrić, S.; Lovrić, M., *Square-Wave Voltammetry, Theory and Application* (Scholz, F., ed.) Springer, Berlin, **2007**.

- (18) Lovrić, M.; Jadreško, D.; Komorsky-Lovrić, S., Theory of square-wave voltammetry of electrode reaction followed by the dimerization of product, *Electrochim. Acta* **2013**, *90*, 226–231. <https://doi.org/10.1016/j.electacta.2012.11.101>
- (19) Osteryoung, J.; Osteryoung, R. A., Theory of square-wave voltammetry for kinetic systems, *Anal. Chem.* **1981**, *53*, 695–701. <https://doi.org/10.1021/ac00227a028>
- (20) Shuman, M. S., Nonunity reaction orders and stationary electrode polarography, *Anal. Chem.* **1969**, *41*, 42–46. doi: 10.1021/ac60270a014
- (21) Mirceski, V.; Guziejewski, D.; Gulaboski, R., Genuine anodic and cathodic current components in cyclic voltammetry, *Sci. Rep.* **2024**, *14*, 17314. <https://doi.org/10.1038/s41598-024-67840-x>
- (22) Dauphin-Ducharme, Ph.; Arroyo-Curras, N.; Kurnik, M.; Ortega, G.; Li, H.; Plaxco, K. W., Simulation-based approach to determining electron transfer rates using square-wave voltammetry, *Langmuir*, **2017**, *33*, 4407–4413. DOI:10.1021/acs.langmuir.7b00359
- (23) Gulaboski, R.; Mirceski, V., Application of voltammetry in biomedicine – Recent achievements in enzymatic voltammetry, *Maced. J. Chem. Chem. Eng.* **2020**, *39*, 153–166. DOI: 10.20450/mjce.2020.2152